

# Experimental Evidence for Exciton Scaling Effects in Self-Assembled Molecular Wires

P.G. Lagoudakis,\* M. M. de Souza, F. Schindler, J. M. Lupton, and J. Feldmann

*Photonics and Optoelectronics Group, Department of Physics and CeNS, Ludwig-Maximilians-Universität,  
80799 Munich, Germany*

J. Wenus and D.G. Lidzey

*Department of Physics and Astronomy, The University of Sheffield, Hicks Building,  
Hounsfield Road, Sheffield S3 7RH, United Kingdom*

(Received 19 July 2004; published 13 December 2004)

Resonant Rayleigh scattering from self-assembled one-dimensional molecular *J*-aggregate wires reveals a distinct dependence of the exciton energy on the width of lateral extension. For the *J* aggregates used in this study, strong in-line dipole coupling leads to a delocalization of the exciton wave function over several molecular units. Polarization dependent measurements of resonantly scattered light from the wires show that the exciton dipole moment is oriented perpendicular to the long axis. The experimental observations can be described by applying a quantization condition to the center of mass motion of the *J*-band exciton in the wires.

DOI: 10.1103/PhysRevLett.93.257401

PACS numbers: 78.67.Lt, 71.35.-y, 78.35.+c

The evolution of low-dimensional inorganic semiconductors has been closely followed by the developments in organic semiconductors. Inorganic semiconductor quantum wells (QWs), wires (QWRs), and dots (QDs) have been the subject of intense studies in the last few decades and the physics of these systems is well understood [1,2]. Conversely, the physical properties of organic semiconductors, and, in particular, the degree of localization of the electronic excitation in organic crystals (Wannier versus Frenkel exciton) have been a subject of debate [3,4]. The most profound evidence of exciton delocalization in molecular quasicrystals has been the observation of superradiant emission from an organic crystal of aggregated dye molecules when compared to that of isolated molecules [5–7]. Delocalization of the electronic excitation allows the investigation of effects of quantum confinement in organic crystals, which in turn pave the way to promising applications in quantum information technology.

There has been considerable controversy over the question whether organic materials can form quantum wire structures. In a few cases, single semiconducting macromolecules, such as polydiacetylenes polymerized in monomeric crystals and some classes of  $\sigma$ -conjugated polymers, exhibit properties of natural quantum wires [8,9]. However, those wires are thought of as true 1D systems with minimal lateral extension, which leads to confinement of the *charge carrier* wave function. In contrast, inorganic quantum wires have a substantial width, which controls the level of confinement of either charge carrier or *exciton* wave function as a whole. Little is known about quantum confinement effects in crystalline molecular assemblies, which could potentially form QWR structures exhibiting lateral confinement. Supramolecular aggregates of cyanine dyes can self-assemble under certain conditions to form ostensible one-

dimensional structures [10,11]. Scanning electron microscopy (SEM), x-ray diffraction, near field scanning optical microscopy, and atomic force microscopy measurements have revealed that these structures resemble cables since they are formed from fibrillation of ordered molecular aggregates surrounded by a thick cladding of more amorphous molecular assemblies [11–14].

In this Letter, we demonstrate that one-dimensional self-assembled molecular *J*-aggregate wires of cyanine dyes exhibit evidence of lateral quantum confinement effects and can therefore be considered as supramolecular QWR structures. We have developed a systematic way of producing thin gelatine films with embedded molecular cyanine *J*-aggregate elongated structures (wires) of variable lengths and widths. We used SEM to characterize the structural configuration of the *J*-aggregate wires, and we observed that the width of these structures varies systematically along the wire. Resonant Rayleigh scattering from single wires reveals a distinct dependence of the *J*-band exciton energy on the width of the lateral confinement. We interpret the observed energy dependence in terms of a lateral quantization of the center-of-mass motion of the exciton in the wire, since the influence of the lateral confinement on the wave functions of the correlated relative motion of the electron and hole is negligible in wide wires. Delocalization of the exciton wave function is attributed to strong in-line dipole-dipole coupling, which is further supported by the experimentally observed alignment of the exciton dipole moments in the direction perpendicular to the wire. We find good agreement between this model and the experiment for a systematic reduction of the active wire width compared to the physical width measured with SEM. We conclude that the physical elongated *J*-aggregate agglomerate consists of a fibril structure, where the individual fibrils give rise to the QWR properties. The scaling of the macroscopic

wire elongation on the micrometer scale with the strength of quantum confinement on the nanometer scale may provide new directions for tuning electronic properties and processes in organic or hybrid optoelectronic devices.

Like most of the cyanine dyes, the material used in this study [15] carries a net positive charge, as shown in the inset of Fig. 1(a). In appropriate solvents, the polarity of the individual molecule, i.e., the monomer, leads to self-association with other molecules and finally to the formation of an extended molecular *J* aggregate, which may have a helical structure for some cyanine dyes [16]. Coupling between the in-line transition dipoles creates a band of delocalized states (excitonic *J* band [17]), which results in a redshifted, narrowed absorption peak compared to the monomer, and a small Stokes shift between the absorption and emission lines [18].

On a macroscopic scale, *J*-aggregates tend to agglomerate, while under certain conditions they can self-assemble to form wires of submicron diameters and of several micrometers length [11]. For the *J* aggregates to form single self-assembled wires the cyanine dye was

dissolved in a gelatine solution in water. The solution was then heated and spin coated onto either glass or indium tin oxide (ITO) coated glass substrates to form optical quality thin gelatine films of dispersed *J*-aggregate wires. Room temperature optical absorption and photoluminescence emission spectra from a thin film of the molecular *J* aggregate on a glass substrate exhibit a Stokes shift of approximately 4 nm [Fig. 1(a)]. We can control the density of these structures through the monomer concentration and the deposition conditions during spin coating, which allows us to perform spectroscopy on a single wire. Using a dark-field microscope, light scattering images from wires of different lengths were obtained. Figure 1(b) shows a collection of different images obtained for various single wires.

To quantify the average physical configuration of the wires, we used SEM on a thin gelatine matrix film prepared on an ITO substrate. It was then possible to image the wires lying on the gelatine-air interface. The lengths of the wires under study are between 2 and 4.5  $\mu\text{m}$ , and their average thicknesses as estimated from SEM images are in the range of 150 to 600 nm. We found a steady increase in the width of the structure with increasing length. Furthermore, we observed that there is a certain trend for the thickness to decrease along the wire towards the ends. A typical SEM image of these structures is shown in Fig. 1(c).

A double microscope was employed to perform resonant Rayleigh scattering spectroscopy. An ultraviolet free white light source was used to illuminate the wires in order to avoid nonresonant excitation of the molecular *J* aggregates. A dark-field condenser of high numerical aperture ( $\text{NA} = 1.2\text{--}1.4$ ) was used for wide angle excitation of single *J*-aggregate wires [19]. Scattered light from a single wire in focus was collected with a second microscope objective ( $\text{NA} = 1.0$ ) and was then spectrally resolved.

Resonant Rayleigh scattering was collected from different cross sections along the *J*-aggregate wires [Fig. 2(a)]. Figure 2(b) shows how the peak emission energy varies over 7 meV for adjacent cross sections along a wire 3  $\mu\text{m}$  in length. The emission energy is higher towards the end of the wire, where it is thinner and its cross sections are therefore smaller, as seen clearly in the reflectivity image of a single wire [Fig. 2(a)]. There is a distinct correlation between the thickness of the wire and the emission energy from the *J*-band exciton in the wire. The observed dependence suggests that spatial confinement of the excitons occurs in the plane perpendicular to the wire and on a scale comparable to the delocalization of its wave function. However, the spread of the wave function in the molecular structure strongly depends on the orientation of the in-line transition dipole moments. It is therefore essential to measure the polarization dependence of the exciton emission, which reflects the transition dipole moment orientation.

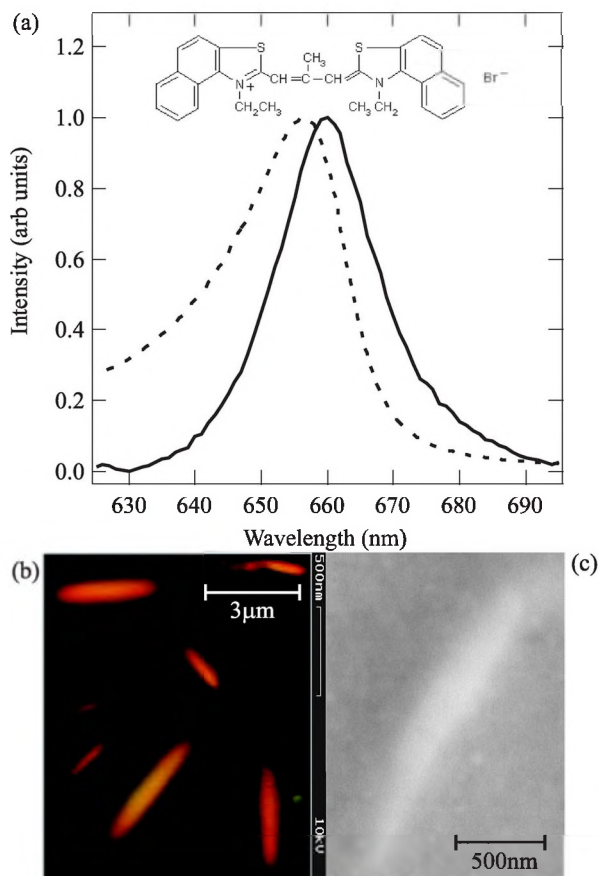


FIG. 1 (color online). (a) Normalised absorption (dashed line) and emission (solid line) spectra of a film of *J*-aggregate wires dispersed in a gelatine matrix. The inset shows the chemical structure of the cyanine dye studied. (b) Light scattering images of single wires of different lengths dispersed in a gelatine matrix. (c) SEM image of a *J*-aggregate self-assembled wire bundle formed at the surface of the gelatine film.

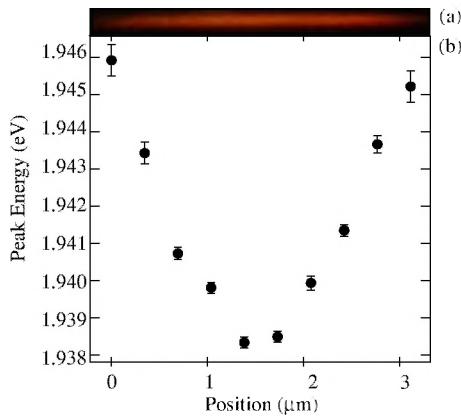


FIG. 2 (color online). (a) Scattering image of a single elongated *J* aggregate of 3  $\mu\text{m}$  length. (b) *J*-band peak energy in dependence of spatial position along the aggregate.

The normalized intensity of the *J*-band exciton as a function of linear polarization angle is shown in Fig. 3(a) (dots). A polarization angle of  $90^\circ$  corresponds to linear polarization parallel to the wire. The dependence fits well with a typical  $\cos^2(\theta)$  polarization curve. The observed polarization dependence clearly exhibits a preferential orientation of the exciton dipole moments in the direction perpendicular to the wire. This observation is in agreement with the helical structural configuration of single supramolecular *J*-aggregate structures of particular cyanine dyes [16,20]. For a helix of small vertical loop separation, the projection of in-line transition dipole moments is mostly perpendicular to the long axis of the helix, as shown in the inset of Fig. 3(a). The residual background of the emission is nonpolarized and therefore attributed to uncoupled monomers.

The observed polarization dependence provides evidence for the physical configuration of the self-assembled molecular wires as sketched in Fig. 3(b). Previous studies

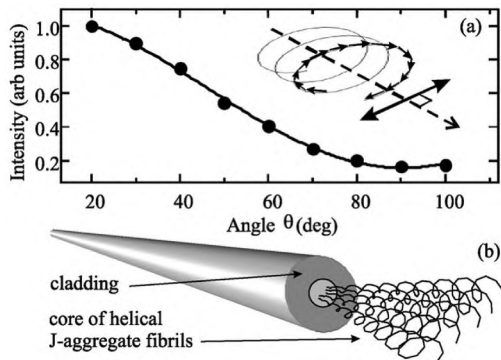


FIG. 3. (a) Normalized intensity of the *J*-band exciton as a function of polarization direction  $\theta$  (dots), together with a  $\cos^2\theta$  fit (solid curve). The polarization angle of  $90^\circ$  corresponds to linear polarization parallel to the wire. The inset shows how a helical arrangement of the monomers leads to the polarization observed. (b) Pictorial structural configuration of the molecular wire.

on the structure of similar wires resolved that the core of the assembly consists of a bunch of *J*-aggregate fibrils parallel to the wire and that the core is covered by a cladding of more amorphous molecular arrangements and monomers, which can be up to 1 order of magnitude thicker than the core [11]. Furthermore, the *J* aggregates have a helical structure and therefore the transition dipoles are aligned perpendicular to the wire, as manifested by the polarization dependence [inset Fig. 3(a)]. It is therefore conceivable that the observed energy dependence in the self-assembled molecular wires of this study can be attributed to lateral quantization of the exciton wave function in the core of the *J*-aggregate wire, with the cladding surrounding the wires forming an infinite potential barrier for the *J*-band excitons in the core of the wires.

Quantization of the electronic transition requires delocalization of the exciton wave function over several molecular units. Although most of the organic *J*-band excitons are strongly localized, *J* aggregates of cyanine dyes have been reported to exhibit an extended delocalization of the exciton wave function over up to 100 molecular units in several experimental studies [6,7]. This apparent deviation from the Frenkel exciton model of organic photoexcitations has been ascribed theoretically to strong in-line dipole-dipole coupling and exciton-optical phonon coupling [6,7,21–23]. Therefore, delocalization of the *J*-band excitons between intramolecular units as well as between intermolecular units of closely neighboring helical *J* aggregates can be justified within the framework of the previous experimental and theoretical studies. Transition dipole coupling is strongest for in-line dipoles; thus the observed polarization dependence further supports the assertion of an extended delocalization of the exciton wave function perpendicular to the wires.

For wires much thicker than the exciton Bohr radius the lateral confinement cannot independently quantize the wave function of the correlated relative motion of the electron and the hole [24]. In this case, dipole-dipole coupling and exciton-optical phonon coupling lead to the spreading of the exciton oscillator strength and therefore delocalization of the *J*-band excitons over several molecular units [6,7,21–23]. For wire widths comparable to the exciton delocalization length, the exciton as a whole is reflected at the lateral boundaries and creates quantized standing waves on a direction perpendicular to the wire axis. The exciton kinetic energy of the center-of-mass (c.m.) motion in the quantized directions is simply given by

$$E_{\text{c.m.}} = \frac{\hbar^2 \pi^2 n^2}{2M_X L_q^2}, \quad n = 0, 1, \dots, \quad (1)$$

where  $M_X$  is the *J*-band exciton effective mass,  $L_q$  is the lateral quantization length, and  $n = 1$ . The effective mass of the *J*-band exciton is approximated with  $M_X = 8m_0$ ,

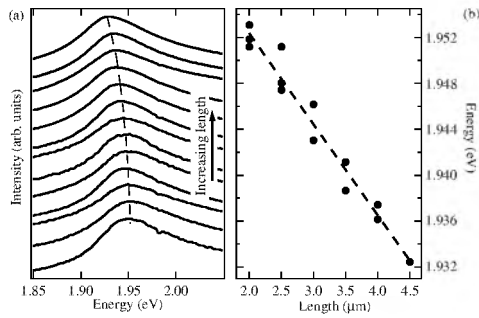


FIG. 4. (a) Resonant Rayleigh scattering spectra from wires of different lengths (wire length increases upwards; spectra offset for clarity). (b) Plot of the peak energy position of the resonant Rayleigh scattering spectra versus wire length. The dashed line is a guide to the eye.

where  $m_0$  is the free electron mass, within the range of values reported in the literature [25]. This approximation leads to a lateral confining length  $L_q$  that varies from 2.5 to 25 nm along the wire and accounts for 99% of the observed energy change. For the particular cyanine *J* aggregate, the calculated lateral confining length corresponds to several molecular units over which delocalization of the *J*-band exciton may occur.

The spatial energy dependence along the long axis of these self-assembled *J*-aggregate structures, as shown in Fig. 2, is observed in most of the wires formed. Figure 4(a) shows resonant Rayleigh scattering spectra from the middle cross section of single wires of different lengths, where the lengths were determined from the dark-field microscope images. The broadening of all spectra towards higher energies is due to residual monomer emission. The peak energy position is plotted in Fig. 4(b). There is a systematic shift of over 20 meV to higher energies for decreasing wire length. The aforementioned physical relation between the length of a wire and its thickness, which was observed in the SEM images, evidently also bears a signature in the optical properties of the wires. The correlation between length and width of the structure therefore allows us to investigate the excitonic confinement effects without requiring accurate knowledge of the nanoscale confinement lengths.

In conclusion, this Letter presents evidence for the quantum confinement of *J*-band excitons in self-assembled molecular wires. A simple model of the center-of-mass quantization of the exciton perpendicular to the wire describes the experimental observations. The phenomena studied here are similar to those observed in inorganic QWRs [26]; however, whereas complex fabrication techniques are required for inorganic structures, organic semiconductors benefit from the versatility of both the choice of precursor materials and the self-assembly based processing procedures. The present study links the fields of both organic and inorganic semiconductor QWRs by demonstrating that quantum confine-

ment effects in organic semiconductors can be controlled by micron-scale structural engineering. The well understood exciton dynamics in inorganic QWRs [27–30] could furthermore provide an elaborate test board of exciton dynamics in organic QWRs. Further x-ray diffraction measurements on these organic wire structures should clarify their actual crystalline properties. Future experiments will test the possibilities of hybrid QWR configurations [31], which could lead to a novel generation of hybrid organic-inorganic optoelectronic devices exploiting both the chemical diversity of organic semiconductors as well as the structural purity of inorganic materials.

We are indebted to the CeNS for the use of the SEM facilities, as well as to W. Stadler and C. Holopirek for excellent technical assistance. Financial support of the EU HYTEC Network, the SFB 486, and the DFG by the Gottfried Wilhelm Leibniz Preis is gratefully acknowledged.

\*Corresponding author.

Electronic address: Pavlos.Lagoudakis@physik.uni-muenchen.de

- [1] Z. I. Alferov, Rev. Mod. Phys. **73**, 767 (2001).
- [2] F. Rossi *et al.*, Rev. Mod. Phys. **74**, 895 (2002).
- [3] A. J. Heeger, Rev. Mod. Phys. **73**, 681 (2001).
- [4] V. M. Axt *et al.*, Rev. Mod. Phys. **70**, 145 (1998).
- [5] R. H. Dicke, Phys. Rev. **93**, 99 (1954).
- [6] F. C. Spano *et al.*, Phys. Rev. Lett. **65**, 211 (1990).
- [7] H. Fidler *et al.*, Phys. Rev. Lett. **66**, 1501 (1991).
- [8] M. Fujiki, Appl. Phys. Lett. **65**, 3251 (1994).
- [9] F. Dubin *et al.*, Phys. Rev. B **66**, 113202 (2002).
- [10] F. F. So *et al.*, Phys. Rev. Lett. **66**, 2649 (1991).
- [11] E. S. Emerson *et al.*, J. Phys. Chem. **71**, 2396 (1967).
- [12] L. Wolthaus *et al.*, Chem. Phys. Lett. **225**, 322 (1994).
- [13] J. E. Maskasky, Langmuir **7**, 407 (1991).
- [14] D. A. Higgins *et al.*, J. Am. Chem. Soc. **118**, 4049 (1996).
- [15] 3,3'-Diethyl-9-methyl-4,5,4',5'-dibenzothiacarbocyanine bromide.
- [16] A. Pawlik *et al.*, J. Phys. Chem. B **101**, 5646 (1997).
- [17] E. D. McRae *et al.*, J. Phys. Chem. **28**, 721 (1958).
- [18] E. E. Jelly, Nature (London) **138**, 1009 (1936); **139**, 631 (1937).
- [19] G. Raschke *et al.*, Nano Lett. **3**, 935 (2003).
- [20] S. Kirstein *et al.*, Chem. Phys. Chem. **1**, 146 (2000).
- [21] M. Orrit *et al.*, Phys. Rev. B **25**, 7263 (1982).
- [22] M. Orrit *et al.*, Phys. Rev. B **34**, 680 (1986).
- [23] E. O. Potma *et al.*, J. Chem. Phys. **108**, 4894 (1998).
- [24] S. Glutsch *et al.*, Phys. Rev. B **47**, 4315 (1993).
- [25] V. F. Kamalov *et al.*, J. Phys. Chem. **100**, 8640 (1996).
- [26] J. Shah, *Ultrafast Spectroscopy of Semiconductors and Nanostructures*, (Springer-Verlag, Berlin, 1996).
- [27] R. Cingolani *et al.*, Phys. Rev. Lett. **67**, 891 (1991).
- [28] D. S. Citrin, Phys. Rev. Lett. **69**, 3393 (1992).
- [29] M. Oestreich *et al.*, Phys. Rev. Lett. **70**, 1682 (1993).
- [30] R. Kumar *et al.*, Phys. Rev. Lett. **81**, 2578 (1998).
- [31] V. I. Yudson *et al.*, Phys. Rev. B **52**, 5543 (1997).